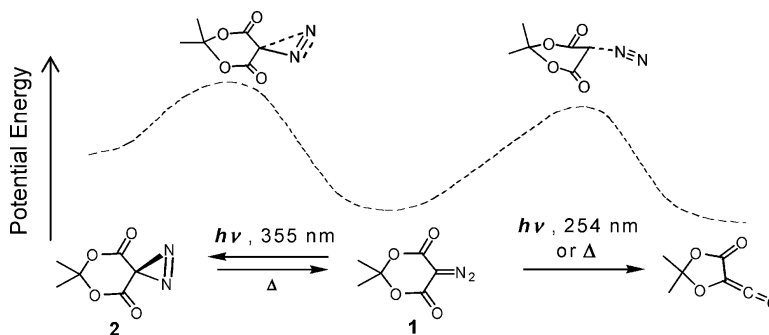


Experimental and Theoretical Investigation of Reversible Interconversion, Thermal Reactions, and Wavelength-Dependent Photochemistry of Diazo Meldrum's Acid and Its Diazirine Isomer, 6,6-Dimethyl-5,7-dioxo-1,2-diaza-spiro[2,5]oct-1-ene-4,8-dione

Aneta Bogdanova, and Vladimir V. Popik

J. Am. Chem. Soc., 2003, 125 (46), 14153-14162 • DOI: 10.1021/ja037637d • Publication Date (Web): 22 October 2003

Downloaded from <http://pubs.acs.org> on March 30, 2009



More About This Article

Additional resources and features associated with this article are available within the HTML version:

- Supporting Information
- Links to the 2 articles that cite this article, as of the time of this article download
- Access to high resolution figures
- Links to articles and content related to this article
- Copyright permission to reproduce figures and/or text from this article

[View the Full Text HTML](#)

Experimental and Theoretical Investigation of Reversible Interconversion, Thermal Reactions, and Wavelength-Dependent Photochemistry of Diazo Meldrum's Acid and Its Diazirine Isomer, 6,6-Dimethyl-5,7-dioxo-1,2-diaza-spiro[2,5]oct-1-ene-4,8-dione¹

Aneta Bogdanova and Vladimir V. Popik*

Contribution from the Center for Photochemical Sciences, Bowling Green State University, Bowling Green, Ohio 43403

Received July 30, 2003; E-mail: vpopik@bgnet.bgsu.edu

Abstract: The photochemical or thermal decomposition of diazo Meldrum's acid (**1**) in methanolic solutions yields ketoester **3a**, the product of the Wolff rearrangement, while products produced from the singlet carbene were not detected. This observation, combined with the analysis of activation parameters for the thermal decomposition of **1**, as well as with the results of DFT B3PW91/6-311+G(3df,2p) and MP2/aug-cc-pVTZ//B3PW91/6-311+G(3df,2p) calculations, allows us to conclude that the Wolff rearrangement of **1** is a concerted process. The outcome of the photolysis of diazo Meldrum's acid depends on the wavelength of irradiation. Irradiation with 254 nm light results in an efficient ($\Phi_{254} = 0.34$) photo-Wolff reaction, while at 355 nm, the formation of diazirine **2** becomes the predominant process ($\Phi_{350} = 0.024$). This unusual wavelength selectivity indicates that Wolff rearrangement and isomerization originate from different electronically excited states of **1**. The UV irradiation of diazirine **2** leads to the loss of nitrogen and the Wolff rearrangement, apparently via a carbene intermediate. This process is accompanied by a reverse isomerization to diazo Meldrum's acid. Triplet-sensitized photolysis of both isomers results in the formation of Meldrum's acid, the product of a formal reduction of **1** and **2**. Mild heating of diazirine **2** produces quantitative yields of diazo Meldrum's acid. The activation parameters for thermal reactions of diazo **1** and diazirine **2** isomers were determined in aqueous and dioxane solutions.

Introduction

The Wolff reaction, the thermal or photochemical transformation of α -diazocarbonyl compounds into carboxylic acid derivatives, is a key step in many laboratory methods, such as the Arndt-Eistert homologation of carboxylic acids,² synthesis of small strained ring systems by ring contraction,^{2a,f,3} preparation of β -ketoacid derivatives,⁴ photoaffinity labeling,⁵ DNA photocleaving,⁶ and nanomachining.⁷ The most important industrial

application of the Wolff rearrangement is found in photolithography, a process used in the production of electronic microchips and integrated circuit boards.⁸ Diazo Meldrum's acid, discussed in this report, is currently under investigation as a potential component of deep-UV photoresists⁹ and mass transfer imaging materials.¹⁰

Mechanistically, the Wolff rearrangement is a complex process that involves several short-lived intermediates.^{11,12} The irradiation or thermolysis of the α -diazocarbonyl compound usually leads to the loss of nitrogen and the formation of an α -carbonylcarbene. This key intermediate in the Wolff rearrangement can exist in two different electronic states, that is,

(1) Preliminary communication: Bogdanova, A.; Popik, V. V. *J. Am. Chem. Soc.* **2003**, *125*, 1456–7.

(2) (a) Regitz, M.; Maas, G. *Diazo Compounds*; Academic Press: Orlando, FL, 1986. (b) Maas, G. In *Methoden der Organischen Chemie (Houben-Weyl)*; Regitz, M., Ed.; Thieme-Verlag: Stuttgart, 1989; Vol. 19b/2, p 1022. (c) Ye, T.; McKervey, A. M. *Chem. Rev.* **1994**, *94*, 1091. (d) Meier, H.; Zeller, K.-P. *Angew. Chem., Int. Ed. Engl.* **1975**, *14*, 32. (e) Jones, M.; Moss, R. A. *Carbenes*; Wiley: New York, 1973. (f) Doyle, M. P.; McKervey, M. A.; Ye, T. *Modern Catalytic Methods for Organic Synthesis with Diazo Compounds*; Wiley-Interscience: New York, 1998; pp 487–534.

(3) (a) Fessner, W.-D.; Prinzbach, H.; Rihs, G. *Tetrahedron Lett.* **1983**, *24*, 5857–5860. (b) Ghosh, A.; Banerjee, U. K.; Venkateswaran, R. V. *Tetrahedron* **1990**, *46*, 3077. (c) Lawton, G.; Moody, C. J.; Pearson, C. J. *J. Chem. Soc., Perkin Trans. 1* **1987**, 877. (d) Moody, C. J.; Pearson, C. J.; Lawton, G. *Tetrahedron Lett.* **1985**, *26*, 3167. (e) Redmore, D.; Gutsche, C. D. *Adv. Alicyclic Chem.* **1971**, *3*, 125.

(4) (a) Cossy, J.; Belotti, D.; Thellend, A.; Pete, J. P. *Synthesis* **1988**, 720. (b) Korobitsyna, I. K.; Nikolaev, V. A. *Zh. Org. Khim.* **1976**, *12*, 1251. (c) Wenstrup, C.; Heilmayer, W.; Kollenz, G. *Synthesis* **1994**, 1219.

(5) Davioud, E.; Fagat, J.; Souque, A.; Rafestin-Oblin, M.-E.; Marquet, A. *J. Med. Chem.* **1996**, *39*, 2860. Somack, R.; Nordeen, S. K.; Eberhardt, N. L. *Biochemistry* **1982**, *21*, 5651.

(6) Nakatani, K.; Maekawa, S.; Tanabe, K.; Saito, I. *J. Am. Chem. Soc.* **1996**, *118*, 10635. Saito, I.; Nakatani, K. *Bull. Chem. Soc. Jpn.* **1996**, *69*, 3007. Wender, P. A.; Touami, S. M.; Alayrac, C.; Philipp, U. C. *J. Am. Chem. Soc.* **1996**, *118*, 6522.

(7) Yang, Y.; Huang, S.; He, H.; Mau, A. W. H.; Dai, L. *J. Am. Chem. Soc.* **1999**, *121*, 10832.

(8) Moreau, W. M. *Semiconductor Lithography*; Plenum Press: New York, 1988. Reiser, A. *Photoreactive Polymers: The Science and Technology of Resists*; Wiley: New York, 1989. Reichmanis, E.; Thompson, L. F. *Chem. Rev.* **1989**, *89*, 1273.

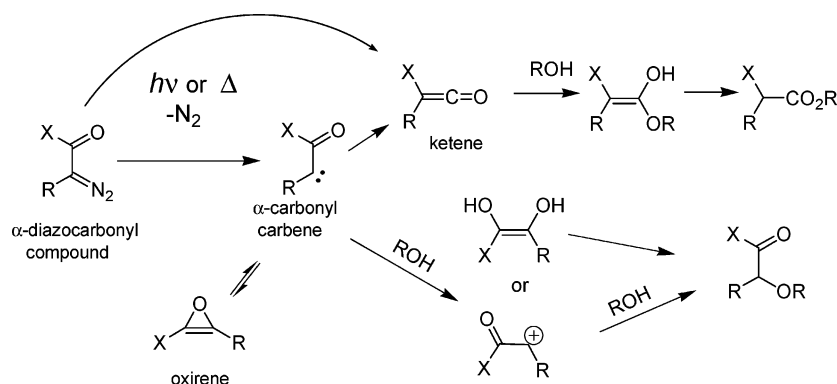
(9) Lippert, T.; Koskelo, A.; Stoutland, P. O. *Mater. Res. Soc. Symp. Proc.* **1996**, *397*, 661. Urano, F.; Oono, K.; Fujie, H. *Eur. Pat. Appl.*, EP 552548 A1 19930728, 1993.

(10) Busman, S. C.; Cuny, G. D.; Zaklika, K. A.; Ellis, R. J. *Eur. Pat. Appl.*, EP 799716 A2 19971008, 1997.

(11) Kirmse, W. *Eur. J. Org. Chem.* **2002**, 2193 and references therein.

(12) Tomioka, H.; Hayashi, N.; Asano, T.; Izawa, Y. *Bull. Chem. Soc. Jpn.* **1983**, *56*, 758.

Scheme 1

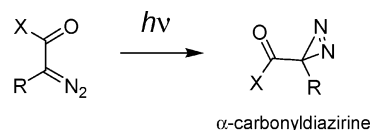


singlet or triplet.^{13–15} Direct photolysis of α -diazocarbonyl compounds is usually dominated by the chemistry of singlet carbenes. α -Carbonylcarbene might also exist in equilibrium with an elusive oxirene.¹⁶ Carbenes are very reactive species and in the presence of water or alcohols undergo rapid O–H insertion reaction.¹⁷ Depending on the electronic properties of the substituent R, this process proceeds via an enol¹⁸ or carbocation¹⁹ intermediate. Alternatively, the α -carbonylcarbene can rearrange to form a ketene. The latter can also be formed directly from the diazo compound by the simultaneous loss of nitrogen and the migration of the substituent X, that is, by the concerted Wolff rearrangement.^{11,20} Ketenes react with nucleophiles to produce corresponding enols, which then rapidly ketonize to yield the final product, carboxylic acid derivatives²¹ (Scheme 1).

The chemistry and properties of the species shown in Scheme 1 have been investigated in detail as their reactivity is a key to understanding and predicting the outcome of reactions of α -diazocarbonyl compounds. One intermediate or byproduct of the Wolff reaction, however, has escaped scrutiny. Thus, α -carbonyldiazirines, cyclic isomers of α -diazocarbonyl compounds, are sometimes isolated in the photolysis of the latter^{22,23} (Scheme 2).

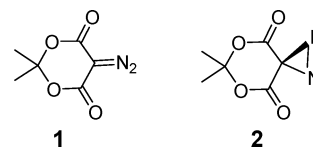
Surprisingly, little is known about the conditions of α -carbonyldiazirines formation, as well as their thermal and photochemi-

Scheme 2



cal reactivity. There are some indications that the yield of α -carbonyl diazirines depends on the wavelength of irradiation of the parent diazo compound,^{22a,23} and they might undergo thermal or photochemical^{22a,e,f} reverse isomerization into the parent diazo compound or lose nitrogen to give an α -carbonylcarbene.^{22a,c,f}

Here, we would like to report the experimental and theoretical investigation of a reversible isomerization of diazo Meldrum's acid (**1**) into the corresponding diazirine, 6,6-dimethyl-5,7-dioxal-1,2-diaza-spiro[2,5]oct-1-ene-4,8-dione (**2**), as well as a comparison of their photochemical and thermal reactivity.



This pair of structural isomers also provides an insight into the unusual reactivity of diazo Meldrum's acid (**1**). Most of the α -diazoesters, for example, closely related diazomalones, produce either a very low yield or no Wolff rearrangement products on photolysis,^{23,24} while for **1**, formation of the corresponding ketene was reported to be the major process in photochemical decomposition.^{24,25} The conventional explanation for this

- (13) Wang, J. L.; Likhtvorik, I. R.; Platz, M. S. *J. Am. Chem. Soc.* **1999**, *121*, 2883. Likhtvorik, I. R.; Zhu, Z.; Tae, E. L.; Tippmann, E.; Hill, B. T.; Platz, M. S. *J. Am. Chem. Soc.* **2001**, *123*, 6061.
- (14) Scott, A. P.; Platz, M. S.; Radom, L. *J. Am. Chem. Soc.* **2001**, *123*, 6069 and references therein.
- (15) McMahon, R. J.; Chapman, O. L.; Hayes, R. A.; Hess, T. C.; Krimmer, H.-P. *J. Am. Chem. Soc.* **1985**, *107*, 7597. Novoa, J. J.; McDouall, J. J. W.; Robb, M. A. *J. Chem. Soc., Faraday Trans. 2* **1987**, *83*, 1629.
- (16) Lewars, E. *Can. J. Chem.* **2000**, *78*, 297 and references therein. Sung, K. S. *Can. J. Chem.* **2000**, *78*, 562. Vacek, G.; Galbraith, J. M.; Yamaguchi, Y.; Schaefer, H. F.; Nobes, R. H.; Scott, A. P.; Radom, L. *J. Phys. Chem.* **1994**, *98*, 8660. Nobes, R. H.; Schaefer, H. F., III; Radom, L. *J. Am. Chem. Soc.* **1994**, *116*, 10159. Lewars, E. G. *Chem. Rev.* **1983**, *83*, 519. Torres, M.; Lown, E. M.; Gunning, H. E.; Strausz, O. P. *Pure Appl. Chem.* **1980**, *52*, 1623–1643. Tomioka, H.; Okuno, H.; Kondo, S.; Izawa, Y. *J. Am. Chem. Soc.* **1980**, *102*, 7123. Zeller, K.-P. *Angew. Chem., Int. Ed. Engl.* **1977**, *16*, 781.
- (17) Kirmse, W. Carbenes and the O–H bond. In *Advances in Carbene Chemistry*; Brinker, U. H., Ed.; JAI Press Inc.: Greenwich, CT, 1994; pp 1–57. Hadel, L. M.; Maloney, V. M.; Platz, M. S.; McGimpsey, W. G.; Scaiano, J. C. *J. Phys. Chem.* **1986**, *90*, 2488. Chiang, Y.; Jefferson, E. A.; Pruszyński, P.; Schepp, N. P.; Wirz, J. *Angew. Chem., Int. Ed. Engl.* **1991**, *30*, 1366.
- (18) Chiang, Y.; Kresge, A. J.; Schepp, N. P.; Xie, R. Q. *J. Org. Chem.* **2000**, *65*, 1175. Chiang, Y.; Jefferson, E. A.; Kresge, A. J.; Popik, V. V.; Xie, R.-Q. *J. Phys. Org. Chem.* **2000**, *13*, 461. Chiang, Y.; Jefferson, E. A.; Kresge, A. J.; Popik, V. V.; Xie, R. Q. *J. Phys. Org. Chem.* **1998**, *11*, 610.
- (19) Schepp, N. P.; Wirz, J. *J. Am. Chem. Soc.* **1994**, *116*, 11749.
- (20) Tidwell, T. T.; Ketenes, J. Wiley: New York, 1976; pp 84–100.
- (21) Kresge, A. J. *Chem. Soc. Rev.* **1996**, *25*, 275–280.

- (22) (a) Rau, H.; Bokel, M. J. *Photochem. Photobiol. A* **1990**, *53*, 311. (b) Ulbricht, M.; Thurner, J. U.; Siegmund, M.; Tomaschewski, G. *Z. Chem.* **1988**, *28*, 102. (c) Torres, M.; Raghunathan, P.; Bourdelande, J. L.; Clement, A.; Toth, G.; Strausz, O. P. *Chem. Phys. Lett.* **1986**, *127*, 205. (d) Laganis, E. D.; Janik, D. S.; Curphey, T. J.; Lemal, D. M. *J. Am. Chem. Soc.* **1983**, *105*, 7457. (e) Miyashi, T.; Nakajo, T.; Mukai, T. *Chem. Commun.* **1978**, 442. (f) Voigt, E.; Meier, H. *Angew. Chem.* **1975**, *87*, 109. (g) Franich, R. A.; Lowe, G.; Parker, J. J. *Chem. Soc., Perkin Trans. 1* **1972**, 2036.
- (23) (a) Livinghouse, T.; Stevens, R. V. *J. Am. Chem. Soc.* **1978**, *100*, 6479. (b) Nikolaev, V. A.; Khimich, N. N.; Korobitsyna, I. K. *Khim. Geterotsikl. Soedin.* **1985**, 321.
- (24) (a) Wang, J.-L.; Toscano, J. P.; Platz, M. S.; Nikolaev, V.; Popik, V. J. *Am. Chem. Soc.* **1995**, *117*, 5477–83. (b) Jones, M., Jr.; Ando, W.; Hendrick, M. E.; Kulczucki, A.; Howley, P. M.; Hummel, K. F.; Malament, D. S. *J. Am. Chem. Soc.* **1972**, *94*, 7469.
- (25) (a) Lippert, T.; Koskelo, A.; Stoutland, P. O. *J. Am. Chem. Soc.* **1996**, *118*, 1551. (b) Winnik, M. A.; Wang, F.; Nivaggioli, T.; Hruska, Z.; Fukumura, H.; Masuhara, H. *J. Am. Chem. Soc.* **1991**, *113*, 9702. (c) Stevens, R. V.; Bisacchi, G. S.; Goldsmith, L.; Strouse, C. E. *J. Org. Chem.* **1980**, *45*, 2708. (d) Kammula, S. L.; Tracer, H. L.; Shelvin, P. B.; Jones, M., Jr. *J. Org. Chem.* **1977**, *42*, 2931.

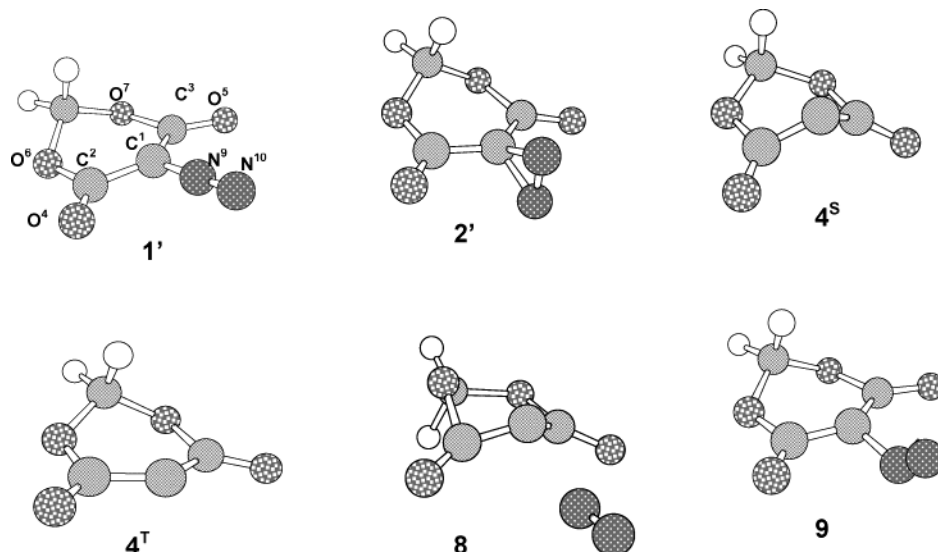
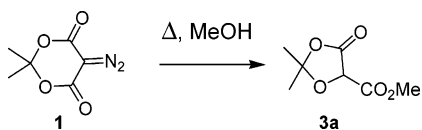


Figure 1. B3PW91/6-311+G(3df,2p) optimized geometries of cyclic diazoester **1'**, diazirine **2'**, singlet **4^S**, and triplet carbene **4^T**, as well as transition states for the concerted Wolff rearrangement **8** and diazo to diazirine isomerization **9**.

Scheme 3



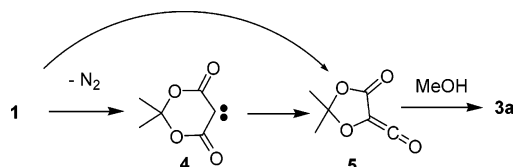
phenomenon is based on the assumption that the irradiation of acyclic α -diazoesters produces α -carbalkoxycarbenes, which do not rearrange due to a low migratory aptitude of oxygen.²⁶ The excitation of diazo Meldrum's acid, on the other hand, results in the concerted Wolff rearrangement that bypasses the carbonylcarbene step (Scheme 1). Diazirines are well-known photochemical precursors of carbenes,²⁷ and the photolysis of α, α' -dicarbonyldiazirine **2** is expected to produce the corresponding carbene.

Results and Discussion

Thermal Reactions of Diazo Meldrum's Acids (1). Diazo Meldrum's acid (**1**) is a relatively stable compound; for example, it melts with an apparent decomposition above 95 °C. We have found that in methanol, water, or 1,4-dioxane solutions, a very slow decomposition of **1** can be observed starting at 60 °C. Because of the high stability of this diazo compound, little is known about products of the thermal decomposition of **1**. The only report known to the authors describes the high temperature pyrolysis of neat diazo Meldrum's acid which resulted in the formation of only the following gaseous products: nitrogen, carbon monoxide, and acetone.^{25d} We found that heating of **1** above 80 °C in neat methanol or in dioxane–methanol mixtures results in the quantitative formation of methyl 2,2-dimethyl-5-oxo-1,3-dioxalane-4-carboxylate (**3a**), the apparent product of the Wolff rearrangement (Scheme 3).

The dediazotization of **1**, in accordance with the general scheme discussed in the Introduction (Scheme 1), could lead

Scheme 4



to the formation of α, α' -dicarbonylcarbene **4** followed by the migration of one of the ring oxygen atoms to the carbene carbon to form α -carbonylketene **5** (Scheme 4). The latter can be also formed in a concerted way directly from **1**. The fact that the carbene insertion product, that is, the 3-methoxy Meldrum's acid, has not been detected in the reaction mixture seems to support the concerted mechanism of the thermal Wolff rearrangement of diazodiester **1**.

Theoretical analysis of the thermal Wolff rearrangement of diazo Meldrum's acid (**1**) was conducted at the B3PW91/6-311+G(3df,2p)//B3PW91/6-311+G(3df,2p) and MP2(full)/aug-cc-pVTZ//B3PW91/6-311+G(3df,2p) levels of theory on the example of 5-diazo-1,3-dioxane-4,6-dione (**1'**, Figure 1). Methyl groups in **1'** were replaced with hydrogen atoms to simplify calculations. In our opinion, this modification should not significantly disturb the relative energies of the species involved in the decomposition of **1**. The optimized geometries of diazodiester **1'**, diazirine **2'**, singlet (**4^S**), and triplet (**4^T**) states of α, α' -dicarbonylcarbene **4'**, transition states for the concerted Wolff rearrangement (**8**), and diazirine isomerization (**9**) are shown in Figure 1. The electronic energies and representative structural parameters of these structures, as well as those of α -carbonylketene **5'**, transition states for the carbene formation (**6**), and carbene to ketene isomerization (**7**), are summarized in Table 1.

The key feature of the stepwise mechanism of the Wolff rearrangement is the formation of the α, α' -dicarbonylcarbene **4'**. The singlet dicarbonylcarbene **4^S** was found to be a real intermediate at the B3PW91/6-311+G(3df,2p) level of theory as it is characterized by the minimum on the potential energy surface (PES) and has no imaginary frequencies. Surprisingly, this species is not planar with the carbene carbon located above the plane of the ring in a boatlike conformation (Figure 1). In

(26) Meier, H.; Zeller, K.-P. *Angew. Chem., Int. Ed. Engl.* **1975**, *14*, 32. Regitz, M.; Maas, G. *Diazo Compounds*; Academic Press: London, 1986; pp 166–198.

(27) Moss, R. A. *Acc. Chem. Res.* **1989**, *22*, 15. Liu, M. T. H.; Stevens, I. D. R. In *Chemistry of Diazirines*; Liu, M. T. H., Ed.; CRC Press: Boca Raton, FL, 1987; Vol. 1, pp 111–160. Doyle, M. P. In *Chemistry of Diazirines*; Liu, M. T. H., Ed.; CRC Press: Boca Raton, FL, 1987; Vol. 2, pp 33–76.

Table 1. Relative Energies and Main Geometrical Parameters of the Equilibrium and Transition Structures Obtained at B3PW91 6-311+G(3df,2p)//B3PW91 6-311+G(3df,2p), MP2 (full) aug-cc-pVTZ //B3PW91 6-311+G(3df,2p) (in Parentheses), and MP2 (full) aug-cc-pVTZ //MP2 (full) 6-311+(d,p) [in Brackets] Levels

	1'	4 ^S + N ₂ ^a	4 ^T + N ₂ ^a	5' + N ₂ ^a	6	7 + N ₂ ^a	8	2'	9
E_{rel}^b (kcal/mol)	0.00	49.19	40.90	-5.88	49.27	49.46	47.84	23.23	53.62
ZPVE corrected		(56.86)	(56.97)	(-3.86)	(55.78)	(57.30)	(48.39)	(22.46)	(60.10)
		[56.70]	[55.39]				[48.05]		
C ¹ -N ⁹ distance/Å	1.319	N/A	N/A	N/A	3.672	N/A	2.217	1.498/1.498	1.540/2.080
N ⁹ -N ¹⁰ distance/Å	1.110	N/A	N/A	N/A	1.095	N/A	1.090	1.190	1.120

^a Energy of the corresponding structure plus energy of a free nitrogen molecule (-109.5176551 (-109.3936875), [-109.39431750] hartree; ZPVE = 3.513 kcal/mol). ^b Energy difference between 1' and the corresponding structure.

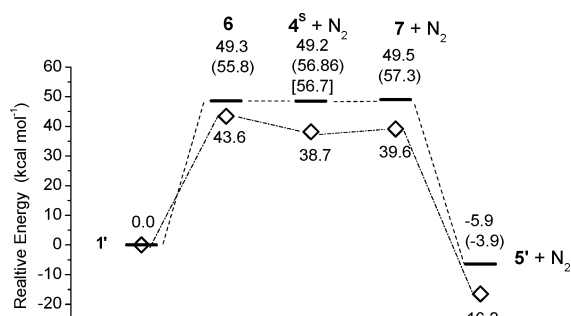


Figure 2. Schematic potential energy profile for the two-step Wolff rearrangement of diazoester 1'. (—) represents electronic energy, and (◇) represents free energy changes.

our opinion, such a geometry provides better overlap of the orbital containing an unshared pair of electrons localized on the carbene atom with the π -system of the carbonyl groups. The triplet state of this carbene (4^T) is predicted to be planar and is 8.3 kcal mol⁻¹ more stable than 4^S. Similar differences in geometry were reported for acyclic α -carbonylcarbenes: in the triplet state, these carbenes are planar, while in the singlet state, the carbonyl group is nearly orthogonal to the carbene plane.¹⁴ It is interesting to note that the correlation-corrected MP2(full) method predicts a much smaller energy gap between the triplet and the singlet state of the carbene 4' than do the density functional calculations (Table 1).

The energy well on the potential energy surface (PES), which corresponds to the singlet carbene 4^S, is very shallow at the B3PW91/6-311+G(3df,2p) level. There is virtually no potential energy barrier for the addition of nitrogen to the carbene. In fact, the single-point energy calculations on MP2 level predict that this carbene is higher in electronic energy than transition state 6 (Figure 2). (Energies shown in the text and in figures correspond to B3PW91/6-311+G(3df,2p) calculations, while values in parentheses were obtained using MP2 (full)/aug-cc-pVTZ //B3PW91/6-311+G(3df,2p) and values in square brackets were obtained using the MP2 (full)/aug-cc-pVTZ //MP2(full)/6-311+G(d,p) method.)

However, the actual activation barrier for the reverse reaction, which includes an entropy term, is much higher; for example, ΔG^\ddagger is 7 kcal mol⁻¹ at 0 °C. A free energy profile for 0 °C calculated at the B3PW91/6-311+G(3df,2p) level for the stepwise Wolff reaction of 1' is shown in Figure 2. It is also interesting to note that the optimized geometry of the transition state, which corresponds to the saddle point on the potential energy surface, is somewhat different from the structure that corresponds to the saddle point on the free energy surface. For example, the C¹-N⁹ distance (numbering of atoms in structures

1'-9 is shown in Figure 1) in 6 is 3.7 Å, while the saddle point on the free energy surface corresponds to a shorter C¹-N⁹ distance of 2.8 Å.

The barrier for the rearrangement of the singlet carbene 4^S to the ketene 5' is predicted by both DFT and MP2 calculations to be very low: below 1 kcal M⁻¹. In accordance with this finding, the geometry²⁸ of the transition state for the rearrangement reaction (7) is very close to that of the singlet carbene 4^S. The only difference is the slight shift of the migrating oxygen atom O.⁶ The C¹-O⁶ distance in 7 is 2.1 Å, while in the starting carbene it is 2.28 Å. We can conclude that α,α' -dicarbonylcarbene 4^S, if ever formed, is an extremely short-lived intermediate with a subpicosecond lifetime immediately collapsing to the ketene 5. This very rapid rearrangement of carbene 4^S predicted by the quantum-mechanical calculations is a noteworthy result. The low yield of the Wolff rearrangement products in the thermal or photochemical decomposition of α -diazoesters is usually explained by the low migratory aptitude of the oxygen atom in an intermediate carbene.^{2d,11} Our results show that there is no intrinsic barrier for the migration of the oxygen atom, at least in the cyclic carbene 4'.

The relaxed PES scan, which follows the shortening of the O⁷-C¹ distance in cyclic diazoester 1', predicts that the concerted Wolff rearrangement, that is, formation of the ketene 5' directly from diazoester 1', is also a feasible process. The geometry of transition state 8 (Figure 1) shows that the concerted Wolff rearrangement of 1' is an asynchronous process. The cleavage of the C¹-N⁹ bond in 8 is almost complete ($l_{\text{C-N}} = 2.22$ Å, Table 1), and the C¹ carbon is shifted from the plane of the molecule similar to carbene 4^S. On the other hand, the C¹-O⁶ distance (1.98 Å) indicates less progress in new bond formation.

The potential energy barrier for the Wolff rearrangement of 1' is 47.8 (48.4) [48.1] kcal mol⁻¹ lower than the barrier for the carbene formation (Figures 2 and 3). In fact, all three methods used in this work, that is, DFT, MP2/DFT, and MP2, place the transition state for the concerted Wolff rearrangement (8) lower in energy than carbene 4'. It has to be noted, however, that frequency calculations predict 6 (carbene formation) to have ca. 16 eu higher entropy than 8. It means that, above a certain temperature, formation of carbene might become the predominant pathway for the deazotization of diazo Meldrum's acid (1). Using the difference in electronic energy between these two states obtained by MP2(full) calculations (ca. 7 kcal/mol), we can estimate this temperature to be ca. 200 °C. The change of

(28) Z-matrices for the species 1'-9 are presented in the Supporting Information.

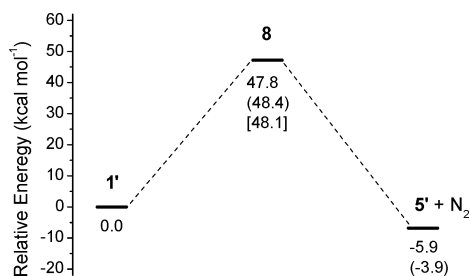


Figure 3. Schematic potential energy profile for the concerted Wolff rearrangement of the diazodiester **1'**.

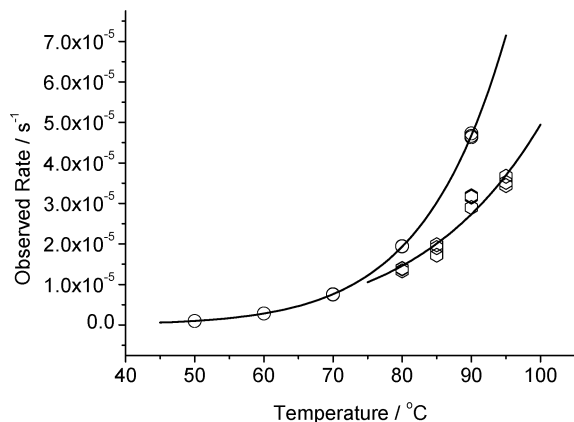


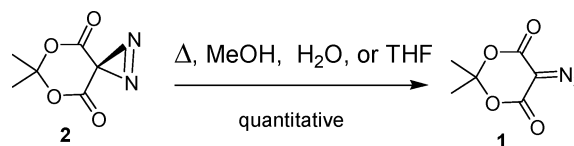
Figure 4. Temperature rate profile for decomposition of **1** in aqueous (circles) and dioxane (hexagons) solutions. The lines shown were drawn using parameters obtained by least-squares fitting of the Eyring equation.

mechanism from concerted to stepwise would be difficult to observe experimentally due to a very low energy barrier separating carbene **4^S** from ketene **5'** (Figure 2). Thus, we were not able to trap carbene **4^S** apparently generated by the photolysis of the diazirine **2** in methanol, but we isolated Wolff rearrangement products instead (vide infra).

Kinetics of the Thermolysis of Diazo Meldrum's Acids (1). The decomposition rates of diazo compound **1** were measured in aqueous and dioxane solutions in the temperature range from 50 to 95 °C. The decay of the substrate was followed by the decrease in absorbance at 250 nm. The data so obtained are summarized in Tables S1 and S2²⁹ and are displayed as the temperature rate profile in Figure 4.

The elongation of the C¹–N⁹ bond that leads to eventual loss of nitrogen and formation of the ketene **5** (or carbene **4^S**) is accompanied by the reduction of conjugation between diazo and carbonyl groups and makes transition state **8** (or **6**) substantially less polar than initial diazo compound **1**. Surprisingly, the rate of decomposition of diazo Meldrum's acid in water is faster than that in less polar dioxane. Analysis of the temperature dependence of the rate of this reaction explains this apparent discrepancy. Least-squares fitting of the data to the Eyring equation³⁰ gives the following activation parameters: $\Delta H^\ddagger = 21.81 \pm 0.13 \text{ kcal M}^{-1}$ and $\Delta S^\ddagger = -18.67 \pm 0.33 \text{ cal M}^{-1} \text{ K}^{-1}$ in aqueous solutions; and $\Delta H^\ddagger = 15.2 \pm 1.7 \text{ kcal M}^{-1}$ and $\Delta S^\ddagger = -37.8 \pm 4.1 \text{ cal M}^{-1} \text{ K}^{-1}$ in dioxane. The enthalpy of activation for the decomposition of **1** in water is, in fact, higher

Scheme 5



than that in dioxane. The interesting feature of the thermal Wolff rearrangement in both solvents is the substantial negative entropy of activation, which is rather unusual for the deazotization reaction. This observation favors the concerted mechanism for the reaction as migration of the O⁶ atom puts substantial constraints on the ring vibrations in transition state **8**, which lowers its vibrational entropy by ca. 15 eu relative to **6**. The negative value of the entropy of activation is abated in aqueous solution due to the higher polarity of the solvent. The polar initial state puts more constraints on the orientation of the dipoles in the solvent shell that are relaxed in the less polar transition state. To check whether strong hydrogen bonding between the partially negatively charged carbonyl oxygen of **1** and water molecules affects the reaction in aqueous solution, we have measured the rate of the decomposition of diazo Meldrum's acid in deuterium oxide at 80 and 90 °C (Table S1²⁹). The solvent isotope effect was found to be $k_H/k_D = 1.30$. The small value of solvent isotope in the normal direction testifies against involvement of strong hydrogen bonds as these bonds become weaker in the transition state and should result in an inverse isotope effect.

The experimental and theoretical results allow us to conclude that the thermal Wolff rearrangement of diazo Meldrum's acid (**1**) is a concerted, albeit asynchronous, process.

Thermal Reactions of Diazirino Meldrum's Acids (2). The thermal stability of 6,6-dimethyl-5,7-dioxo-1,2-diaza-spiro[2,5]-oct-1-ene-4,8-dione, the diazirino Meldrum's acid (**2**), is substantially lower than that of diazo isomer **1**. Mild heating of **2** results in quantitative isomerization into diazo Meldrum's acid (**1**) (Scheme 5).³¹

The theoretical analysis of the reactivity of diazirine **2'** (analogue of **2** without methyl groups in 6-position) showed that the lowest energy barrier leads to reverse isomerization into diazodiester **1'**. We were unable to locate a saddle point on PES that links **2'** with carbene **4'**. In the example of simpler α -carbonyl diazirine, the 2-diazirinoacetic acid, we have conducted a relaxed 3-D PES scan in terms of both C–N distances³² and found that any process other than isomerization proceeds through a much higher energy barrier. The progress of the **2' → 1'** isomerization was explored by both the restricted and the unrestricted DFT method. No intermediates in this reaction were found in either case.

The optimized geometries of diazirine **2'** and the transition state for isomerization reaction (**9**) are shown in Figure 1, with corresponding energies presented in Table 1. It is interesting to note that the ring opening of diazirine proceeds with a nonequivalent elongation of both C–N bonds. In the transition

(29) Supporting Information; see paragraph at the end of this paper regarding availability.

(30) The nonlinear least-squares fitting calculations were conducted using Origin 6.0 by Microcal. The transmission coefficient in the Eyring equation was set to unity.

(31) This process is so efficient that it was used to develop TLC plates. Diazirine **2** has virtually no absorbance at 254 nm and is therefore invisible on TLC plates with conventional fluorescent indicator. Heating the plate in an oven at ca. 100 °C for 1 min converts **2** into diazo Meldrum's acid (**1**), which gives an intense dark spot under UV lamp.

(32) Bogdanova, A.; Popik, V. Abstracts of Papers, 224th ACS National Meeting, Boston, MA, August 18–22, 2002.

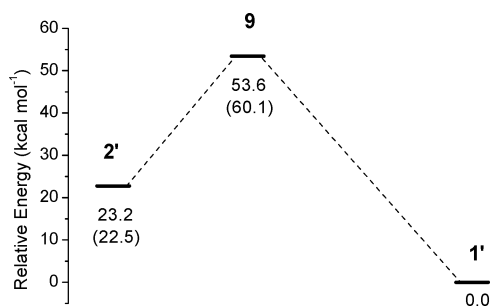


Figure 5. Schematic potential energy profile for the isomerization of α,α -dicarbonyldiazirine **2**.

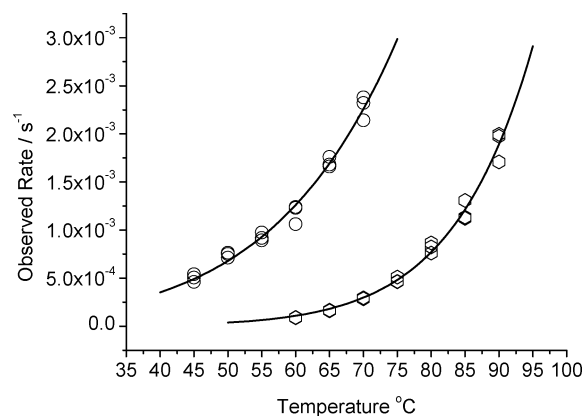


Figure 6. Temperature rate profiles for the isomerization of diazirine **2** aqueous (circles) and dioxane (hexagons) solutions. The lines shown were drawn using parameters obtained by least-squares fitting of the Eyring equation.

state for the isomerization reaction (**9**), corresponding lengths are 1.54 and 2.08 Å versus 1.50 Å in diazirine **2'** and 1.32 Å in diazo compound **1'**. This fact might be considered as evidence of diazirine to diazo isomerization occurring via formation of the carbene followed by the reaction of the latter with N_2 . The geometry of the transition state for the isomerization reaction **9**, however, is very different from that of carbene **4'**; that is, C^1 lies in the plane of the ring (compare **9** with **8** and **4**^S). The potential energy barrier for the diazirine isomerization in the gas phase is predicted to be 30.4 (37.6) kcal/mol (Figure 5). The barrier for the reverse reaction, isomerization of the diazo compound **1'** into diazirine, is 53.6 (60.1) kcal/mol, which is much higher than the activation energy of the Wolff rearrangement. This observation allows us to conclude that the thermal isomerization of diazo Meldrum's acid (**1**) to diazirine (**2**) cannot compete with the loss of nitrogen.

Kinetics of the Thermal Isomerization of Diazirino Meldrum's Acids (2). Rates of the isomerization of diazirine **2** were measured in aqueous and dioxane solutions in the temperature range from 45 to 70 °C in water and from 60 to 90 °C in dioxane. The progress of this reaction was followed by an increase in absorbance at 250 nm due to the formation of diazo Meldrum's acid (**1**). The data so obtained are summarized in Tables S3 and S4²⁹ and are displayed as the temperature rate profile in Figure 6.

The polarity of the solvent has a profound effect on the rate of this reaction. The isomerization of the diazirine **2** is more than 10 times faster in water than in dioxane. Least-squares fitting of the data gives the following activation parameters: $\Delta H^\ddagger = 12.58 \pm 0.52$ kcal M^{-1} and $\Delta S^\ddagger = -34.3 \pm 1.4$ cal

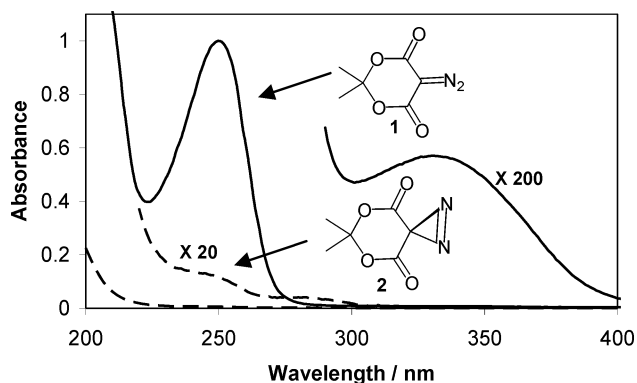
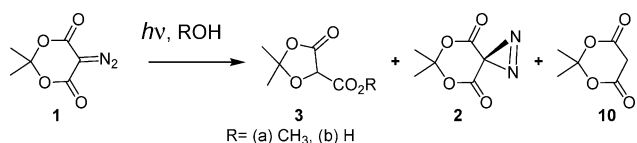


Figure 7. UV spectra of ca. 0.0001 M solutions of diazo Meldrum's acid (**1**, solid line) and diazirine **2** (dotted line) in methanol.

Scheme 6



$M^{-1} K^{-1}$ in aqueous solutions; and $\Delta H^\ddagger = 22.20 \pm 0.98$ kcal M^{-1} and $\Delta S^\ddagger = -10.2 \pm 2.4$ cal $M^{-1} K^{-1}$ in dioxane.

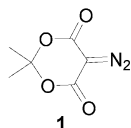
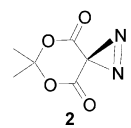
The isomerization of diazirine **2** into diazo Meldrum's acid is accompanied by a substantial increase in the polarity of the molecule. For example, the ESP charge on the N^9 atom calculated by the DFT method rises from -0.001 in the starting diazirine **2** to $+0.226$ in the transition state **9**, and then to $+0.529$ in the diazo isomer. Stabilization of the polar transition state in water results in a 10 kcal M^{-1} lower enthalpy of activation than that in less polar dioxane. The negative entropy of activation of the isomerization reaction is probably due to the solvent effects. In fact, DFT calculations predict an insignificant entropy of activation for this reaction in the gas phase, that is, below 1.0 cal $mol^{-1} K^{-1}$. Apparently, the increased charge separation in the transition state requires a substantial reorganization of the solvent shell, thus resulting in a negative entropy of activation. This effect is stronger in an aqueous solution due to the higher polarity of solvent molecules.

Photochemistry of Diazo (1) and Diazirino Meldrum's Acids (2). The UV spectrum of diazo Meldrum's acid (**1**) has a strong absorbance at 248 nm and a much weaker band at 329 nm (Figure 7). The position of these absorbance bands is virtually independent from the polarity of the solvent. No fluorescence or phosphorescence could be detected at room temperature in solutions of **1** using 254 and 330 nm excitation light. This fact indicates that a fast nonradiative depopulation of excited states takes place. The UV spectrum of isomeric diazirine **2** is very different; it shows only two weak shoulders on the tail of the short-wavelength band at ca. 244 nm and at ca. 284 nm (Figure 7).

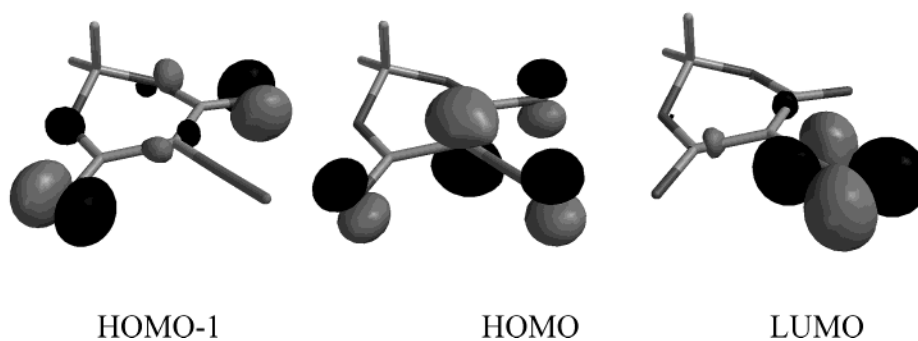
Direct photolysis of the methanolic or aqueous solution of diazo Meldrum's acid (**1**) results in the formation of two major products: ketoacid **3b** or a corresponding ester **3a**, the product of the Wolff rearrangement, and diazirine **2**, the product of isomerization of the starting diazo compound (Scheme 6). Small amounts of Meldrum's acid (**10**) were also detected in the reaction mixtures.

The triplet-sensitized photolysis of **1** in methanol, on the other hand, results in the quantitative formation of Meldrum's acid

Table 2. Results of Low Conversion Photolyses of Diazo Meldrum's Acid (**1**) and Diazirine (**2**) in Methanol at Different Wavelengths

	Product	wavelength of irradiation λ (nm)					
		254	254 / triplet sensitized	266 ^a	300	350	355 ^a
		Fraction in Products Mixture					
 1 Quantum yield	2	0.065	0	0.17	0.17	0.55	0.94
	3a	0.91	0	0.83	0.81	0.42	< 0.06
	10	0.025	1	^b	0.02	0.03	^c
	Quantum yield	0.34				0.0245	
 2	1	0.04	0		0.44	0.36	
	3a	0.93	0		0.56	0.63	
	10	0.02	1 ^d		0.002	0.01	

^a Monochromatic irradiation using the frequency up-converted output of the Nd:YAG laser; 20–30% conversion. ^b Traces. ^c Not detected. ^d In 2-propanol.

**Figure 8.** Frontier molecular orbitals of diazo Meldrum's acid (**1**).

(**10**). This observation is in line with the accepted mechanism of the photochemical reduction of α -diazocarbonyl compounds through a triplet carbonylcarbene intermediate.¹¹ The Wolff rearrangement-to-isomerization product ratio strongly depends on the wavelength of irradiation. Table 2 shows the relative yield of compounds **2**, **3a**, and **10** formed in the photolysis of diazo Meldrum's acid at different wavelengths. Product ratios were measured at low conversion (ca. 10%) to ensure that these values were not affected by secondary photochemistry.

UV irradiation of diazo Meldrum's acid (**1**) with the wavelength close to λ_{\max} of the major absorbance band results mostly in the Wolff rearrangement and formation of ketoester **3a**. At longer wavelengths, isomerization of **1** into diazirine **2** becomes more pronounced, and at 350 nm diazirine becomes the major product. The wavelength dependence of diazo Meldrum's acid photoreactions becomes even more evident when a source of monochromatic light is employed. Thus, irradiation of **1** in methanol with the frequency tripled output of the Nd:YAG laser (355 nm) produces diazirine **2** in high yield, and only traces of ketoester **3a** were observed. The 254 and 350 nm photolyses of diazo Meldrum's acid differ not only in the major photoproduct but also in the quantum yields (Table 2). Irradiation into the major absorbance band of **1** results in a chemical transformation 14 times more efficiently than irradiation into the weaker band.

The most long-wave absorbance band in the UV spectrum of diazo Meldrum's acid apparently corresponds to the excitation

of **1** to the lowest singlet excited state (S_1) by HOMO \rightarrow LUMO transition. The HOMO of diazo Meldrum's acid (**1**) is a p-type orbital, which is mainly localized on the carbon of the diazocarbonyl group and is orthogonal to the plane of the diazocarbonyl fragment. The LUMO is a π^* orbital of N=N bond, which lies in that plane (Figure 8). Thus, HOMO to LUMO transition is a forbidden process due to poor orbital overlap. The TD-B3PW91/6-311++G(3df,2p) calculations support this conclusion, predicting that the HOMO \rightarrow LUMO transition occurs at $\lambda_{\max} = 353$ nm in the gas phase and is, in fact, forbidden. The low extinction coefficient of the 329 nm band in the UV spectrum of diazo Meldrum's acid agrees well with this assignment.

The short-wavelength photolysis of diazo Meldrum's acid results in the formation of a higher excited state, most probably S_2 . The major component of the latter excitation, according to time-dependent DFT calculations, is the HOMO-1 \rightarrow LUMO transition. The HOMO-1 is a nonbonding orbital, which has its largest coefficients on carbonyl oxygens and lies in the plane of the diazocarbonyl fragment. This orbital has an efficient in-phase overlap with LUMO (Figure 8). A good quantum yield ($\Phi_{254} = 0.34$) observed in 254 nm photolysis of **1** indicates that a higher excited state of diazo Meldrum's acid undergoes an extremely rapid loss of nitrogen. For the latter reaction to compete efficiently with an internal conversion, it should proceed at a rate of 10^{12} s^{-1} or faster.³³ The laser flash photolysis

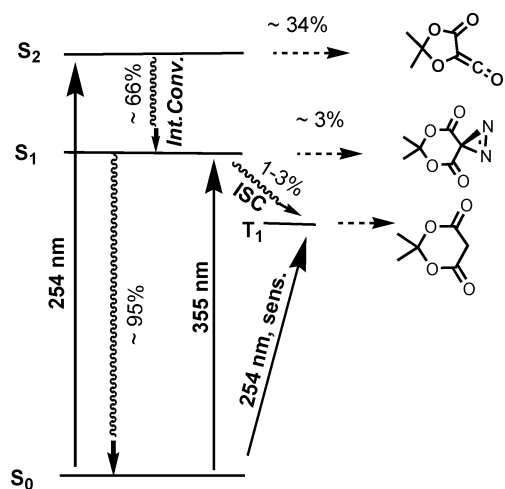


Figure 9. Schematic diagram of process involved in the photochemistry of diazo Meldrum's acid.

of **1** conducted at 248 nm using a KrF laser demonstrated that the formation of a corresponding ketene was complete during the laser pulse (ca. 20 ns).³⁴ This allows us to estimate the lower rate limit for the photo-Wolff rearrangement of **1** at 10^8 s^{-1} .

The summary of processes involved in the photochemistry of diazo Meldrum's acid is represented in Figure 9. The short-wavelength irradiation of **1** populates mainly the S_2 excited state. One-third of the molecules at this level lose nitrogen and eventually form the Wolff rearrangement products. The rest of the molecules undergo an internal conversion to S_1 , participation of which is evident from the formation of small amounts of diazirine **2**, before falling onto the ground state surface. The much higher quantum yield of 254 nm photolysis than that of 350 nm provides an argument against the formation of a Wolff rearrangement product from "hot" S_1 molecules.

Irradiation into a weak long-wavelength band of diazo Meldrum's acid populates the lowest excited state S_1 . The fact that no fluorescence or phosphorescence was observed suggests that thermal deactivation of the lowest singlet excited state to the ground state is a very rapid process. This conclusion agrees with a low quantum yield ($\Phi_{350} = 0.025$) of phototransformation of **1** at 350 nm, indicating that only a small fraction of S_1 population, below 3%, undergoes isomerization into diazirine **2**. We believe that diazirine formation occurs from the S_1 excited state rather than from the "hot" ground state as a thermal reaction of **1** does not produce diazirine **2**, and DFT calculations predict isomerization to be much slower than the Wolff rearrangement (vide supra). Benzophenone-sensitized photolysis apparently populates the lowest triplet excited state of **1**, which loses nitrogen to produce a triplet carbene. The latter undergoes double hydrogen abstraction to give Meldrum's acid (**10**). Traces of **10** found in direct photolyses of **1** are apparently due to the low efficiency intersystem crossing yielding a triplet excited state of **1**.

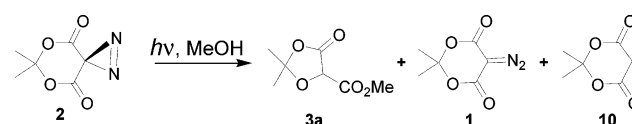
Singlet-Triplet Equilibrium of α,α -Dicarbonyl Carbene

4. DFT and MP2 calculations discussed above show that a singlet carbene 4^S has virtually no barrier for the rearrangement into ketene **5**. The complete absence of the Wolff rearrangement products in sensitized photolysis thus indicates that spin



Figure 10. Formation of diazo Meldrum's acid (**1**) in 300 nm photolysis of diazirine **2** in methanol.

Scheme 7



equilibration of triplet carbene 4^T proceeds much slower than its reaction with methanol. The rate of hydrogen abstraction by triplet carbenes from methanol is usually on the order of $1-5 \times 10^6 \text{ M}^{-1} \text{ s}^{-1}$.³⁵ This value allows us to estimate the lower limit of the activation barrier for intersystem crossing of 4^T into 4^S as 6–7 kcal/mol. Such a rather high barrier can be explained by the necessity for geometrical changes accompanying interconversion.

UV irradiation of diazirino Meldrum's acid (**2**) results in processes similar to that observed in the photolysis of its diazo isomer: Wolff rearrangement producing ketoester **3a**, isomerization to diazo Meldrum's acid (**1**), and formal reduction to **10** (Scheme 7).

The composition of product mixtures in the photolysis of diazirine **2** also depends on the wavelength of irradiation. This dependence, however, is less pronounced: the ketoester **3a** is always the major product, while the yield of diazo compound **1** increases at longer wavelength (Table 2). The results of low conversion photolyses (ca. 10%) of diazirino Meldrum's acid (**2**) allow us to conclude that ketoester **3a** is formed directly from α,α' -dicarbonyl diazirine **2**, rather than from initially formed **1**. The results of photolysis at 300 nm are especially indicative as diazirine **2** and diazo Meldrum's acid (**1**) have similar extinction coefficients (19 and $23 \text{ M}^{-1} \text{ cm}^{-1}$ correspondingly) at this wavelength. The decomposition of the diazo compound formed by isomerization of starting diazirine becomes noticeable only at conversions above 30% (Figure 10). Formation of ketoester **3a** early in the reaction indicates that this product is formed directly from diazirine **2**.

The Wolff rearrangement of diazirine **2** apparently proceeds via a dicarbonyl carbene. The absence of O–H insertion products, on the other hand, indicates an extremely short lifetime of this intermediate, which agrees well with the results of quantum-mechanical calculations (vide supra). The rate of reaction of structurally similar dicarbomethoxycarbene with methanol is $1.5 \times 10^9 \text{ M}^{-1} \text{ s}^{-1}$.^{24a} This value allows us to estimate the lower rate limit for the Wolff rearrangement of

(33) Turro, N. J. *Modern molecular photochemistry*; Benjamin/Cummings Pub. Co.: Menlo Park, CA, 1978.

(34) Kresge, A. J.; Popik, V. V. *ECTOC-1*, June, 1995.

(35) Hadel, L. M.; Maloney, V. M.; Platz, M. S.; McGimpsey, W. G.; Scaiano, J. C. *J. Phys. Chem.* **1986**, *90*, 2488.

the cyclic dicarbonyl carbene at 10^{11} s^{-1} . We also cannot exclude the possibility that photochemical isomerization of diazirine **2** produces "hot" molecules of diazo Meldrum's acid, which then undergo thermal Wolff rearrangement.

Conclusions

The unique wavelength selectivity of the diazo Meldrum's acid photochemistry, as well as the wavelength-dependence of quantum yield, allows us to conclude that isomerization of **1** to diazirine **2** takes place from the lowest singlet excited state, while the Wolff rearrangement originates from the higher excited state. The rate of the diazo group C–N bond cleavage in the latter should be on the order of 10^{12} s^{-1} to be able to compete with internal conversion. The experimental data and quantum-mechanical calculations indicate that the Wolff rearrangement of diazo Meldrum's acid is a concerted process. The UV irradiation of α,α -diazirine **2** also results in the Wolff rearrangement, apparently via the singlet dicarbonylcarbene intermediate **4^S**. According to density functional and MP2 calculations, the carbene-to-ketene isomerization proceeds with insignificant activation energy. Thermolysis of the diazirine **2** results in a smooth electrocyclic ring opening and isomerization to the diazo form.

Experimental Section

General Procedures. NMR spectra were recorded on a Varian Unity+ 400 (200 MHz for ^1H and 100 MHz for ^{13}C) or Varian Gemini 200 (200 MHz for ^1H and 50 MHz for ^{13}C) spectrometer. All NMR spectra were recorded in CDCl_3 and referenced to TMS. FT-IR spectra were recorded on a Thermo Nicolet IR200 spectrometer. UV–vis spectra were obtained on a Cary-300 Bio spectrophotometer. Melting points are uncorrected. Purification of products by column chromatography was performed using 40–63 μm silica gel. Tetrahydrofuran was distilled from sodium/benzophenone ketyl; dioxane, ether, and hexanes were distilled from sodium. Reagents were obtained from Aldrich and used as received unless otherwise noted.

Photolytic Experiments. Analytical photolyses were performed by irradiation of ca. 10^{-4} M solutions of diazo compound **1** or diazirine **2** in a 1 cm quartz cell using a RMR-600 Rayonet photochemical reactor equipped with a carousel and three sets of eight lamps with λ_{max} of emission at 254, 300, or 350 nm. Monochromatic irradiations at 266 and 355 nm were conducted using frequency tripled or quadrupled output of a Q-switched Nd:YAG laser. Reaction mixtures were then analyzed by HPLC. Pure samples of **1**, **2**, **3a**, and Meldrum's acid (**10**) were used as a reference and to calibrate the HPLC detector. Preparative photolyses were conducted by the irradiation of methanolic solutions of ca. 100 mg of substrates using a 16-lamp (with $\lambda_{\text{emission}} = 254$ or 350 nm) Rayonet photochemical reactor and quartz vessel equipped with an immersible cooling finger. The consumption of starting material was followed by TLC. Determination of the quantum yield was performed using a ferrioxalate chemical actinometer.³⁶ The triplet-sensitized photolyses of **1** and **2** were conducted using benzophenone as a sensitizer in thoroughly degassed solutions in methanol or 2-propanol. The concentration of benzophenone was adjusted to achieve sensitizer absorbance at 254 nm 10 times higher than that of the substrate. The sample of diazirine **2** was purified using preparative HPLC before every photolytic experiment. This treatment was necessary to remove minor impurities of diazo Meldrum's acid accumulated during storage.

Kinetics. Rate measurements were performed using a Carry-300 Bio UV–vis spectrometer equipped with a thermostatable cell holder.

Substrate concentrations in the reacting solutions were ca. 10^{-4} M , and the temperature of these solutions was controlled with 0.05 °C accuracy. Reactions were monitored by following the changes of absorbance of diazo Meldrum's acid (**1**) at 250 nm. Observed first-order rate constants were calculated by least-squares fitting of a single-exponential function. At temperatures above 60 °C, where isomerization of **2** was accompanied by a very slow but pronounced decomposition of product **1**, the double exponential function was used.

Theoretical Procedures. Quantum-mechanical calculations were carried out using the Gaussian 98 program.³⁷ Levels of theory examined range from hybrid B3PW91^{38,39} density functional theory calculations with the 6-311+G(3df,2p)⁴⁰ basis sets to high level composite procedures including MP2(full)/aug-cc-pVTZ //B3PW91/6-311+G(3df,2p) and MP2(full)/aug-cc-pVTZ //MP2(full)/6-311+G(d,p). For all of the density functional theory calculations, zero-point vibrational energy (ZPVE) corrections, required to correct the raw relative energies to 0 K, were obtained from the B3PW91/6-311+G(3df,2p) method. Analytical second derivatives were computed to confirm each stationary point as a minimum by yielding zero imaginary vibrational frequencies for the intermediates and one imaginary vibrational frequency for each transition state. These frequency analyses are known to overestimate the magnitude of the vibrational frequencies. Therefore, we scaled the corresponding ZPVE by 0.9772.⁴¹ Initial geometry optimization, IRC calculations for transition states, and relaxed scans of potential energy surfaces were conducted at the B3PW91/6-31+G(d,p) level. The vertical excitation energies were evaluated using the random phase approximation for a time-dependent DFT calculation method,⁴² at the TD-B3PW91/6-311++G(3df,2p) level.

Materials. 5-Diazo-2,2-dimethyl-1,3-dioxane-4,6-dione (diazo Meldrum's acid, **1**) was prepared in 54% yield by the diazotransfer reaction^{2a} from *N-p*-acetamidobenzenesulfonyl azide to Meldrum's acid. Mp 93–95 °C (lit.⁴³ 92–93 °C). ^1H NMR (200 MHz, CDCl_3 , δ /ppm): 1.79 (s). ^{13}C (50 MHz, CDCl_3 , δ /ppm): 26.6, 106.9, 156.2. IR (CCl_4 , cm^{-1}): 2145 (s), 1733 (vs). UV (MeOH, λ_{max} , nm/log ϵ): 248/4, 329/1.42.

6,6-Dimethyl-5,7-dioxo-1,2-diaza-spiro[2,5]oct-1-ene-4,8-dione (Diazirino Meldrum's Acid, 2). A solution of 1 g (5.9 mmol) of diazo compound **1** in 140 mL of a THF–water mixture (8:1) was irradiated at 8 °C for 24 h in a Rayonet photoreactor equipped with 16 350 nm lamps. THF was removed in a vacuum at 0 °C, and colorless crystals precipitated from water. Crystalline product (480 mg) was dissolved in chloroform, washed twice with saturated sodium carbonate and water, dried over MgSO_4 , and solvent was removed in a vacuum at room temperature to give 322 mg (32%) of diazirine **2**. Mp 85 °C (lit.^{23a} 82–84 °C). ^1H NMR (200 MHz, CDCl_3 , δ /ppm): 1.99 (s). ^{13}C (100 MHz, CDCl_3 , δ /ppm): 27.9, 107.6, 161.5.

Methyl 2,2-Dimethyl-5-oxo-1,3-dioxalane-4-carboxylate (3a). A solution of 300 mg (1.8 mmol) of **1** in 50 mL of methanol was irradiated

(36) Murov, S. L.; Carmichael, I.; Hug, G. L. *Handbook of Photochemistry*; Marcel Dekker: New York, 1993; p 299.

- (37) Frisch, M. J.; Trucks, G. W.; Schlegel, H. B.; Scuseria, G. E.; Robb, M. A.; Cheeseman, J. R.; Zakrzewski, V. G.; Montgomery, J. A., Jr.; Stratmann, R. E.; Burant, J. C.; Dapprich, S.; Millam, J. M.; Daniels, A. D.; Kudin, K. N.; Strain, M. C.; Farkas, O.; Tomasi, J.; Barone, V.; Cossi, M.; Cammi, R.; Mennucci, B.; Pomelli, C.; Adamo, C.; Clifford, S.; Ochterski, J.; Petersson, G. A.; Ayala, P. Y.; Cui, Q.; Morokuma, K.; Malick, D. K.; Rabuck, A. D.; Raghavachari, K.; Foresman, J. B.; Cioslowski, J.; Ortiz, J. V.; Stefanov, B. B.; Liu, G.; Liashenko, A.; Piskorz, P.; Komaromi, I.; Gomperts, R.; Martin, R. L.; Fox, D. J.; Keith, T.; Al-Laham, M. A.; Peng, C. Y.; Nanayakkara, A.; Gonzalez, C.; Challacombe, M.; Gill, P. M. W.; Johnson, B. G.; Chen, W.; Wong, M. W.; Andres, J. L.; Head-Gordon, M.; Replogle, E. S.; Pople, J. A. *Gaussian 98*; Gaussian, Inc.: Pittsburgh, PA, 2001.
- (38) Becke, A. D. *J. Chem. Phys.* **1993**, *98*, 5648.
- (39) Burke, K.; Perdew, J. P.; Wang, Y. In *Electronic Density Functional Theory: Recent Progress and New Directions*; Dobson, J. F., Vignale, G., Das, M. P., Eds.; Plenum Press: New York, 1998. Perdew, J. P.; Wang, Y. *Phys. Rev.* **1992**, *B45*, 13244.
- (40) Hehre, W. J.; Radom, L.; Schleyer, P. v. R.; Pople, J. A. *Ab Initio Molecular Orbital Theory*; John Wiley & Sons: New York, 1986.
- (41) Scott, A. P.; Radom, L. *J. Phys. Chem.* **1996**, *100*, 16502.
- (42) Casida, M. E.; Jamorski, C.; Casida, K. C.; Salahub, D. R. *J. Chem. Phys.* **1998**, *108*, 4439.
- (43) Green, G. M.; Peet, N. P.; Metz, W. A. *J. Org. Chem.* **2001**, *66*, 2509.

at 10 °C in a mini-Rayonet photoreactor equipped with 254 nm lamps for 4 h. Solvent was removed under vacuum, and the residue was redissolved in ether and washed with saturated sodium carbonate solution. The organic layer was dried over MgSO₄, and solvent was removed in a vacuum. The reaction mixture was separated using preparative TLC on silica gel to give 171 mg (67%) of ester **3a** as colorless oil. ¹H NMR (200 MHz, CDCl₃, δ/ppm): 1.64 (s, 3H), 1.71 (s, 3H), 3.87 (s, 3H), 4.98 (s, 1H), lit.²³

The same compound was also obtained by thermolysis of the methanolic solution of **1** in a pressure vessel overnight at 120 °C. The ¹H NMR spectrum of reaction mixture obtained after removal of solvent showed the presence of only **3a**.

2,2-Dimethyl-5-oxo-1,3-dioxalane-4-carboxylic acid (3b). A solution of 200 mg (1.2 mmol) of **1** in 50 mL of a THF–water mixture (5:1) was irradiated at room temperature in a Rayonet photoreactor equipped with 254 nm lamps until complete decomposition of diazo compound was achieved (ca. 40 min). THF and water were removed in a vacuum at 30–40 °C, and the residue was redissolved in methylene

chloride and dried over Na₂SO₄. The ¹H spectrum of crude product showed that it contained mainly target ketoacid **3b** with ca. 10% impurity of Meldrum's acid (**10**). Preparative TLC purification of the crude product gave 144 mg (77%) of pure **3b** as colorless oil, which slowly crystallizes on standing. ¹H NMR (200 MHz, CDCl₃, δ/ppm): 1.68 (s, 3H), 1.71 (s, 3H), 5.00 (s, 1H), 9.05 (broad s), lit.²³ UV (H₂O, λ_{max}, nm/log ε): 270/3.1.

Acknowledgment. We are grateful to the National Institutes of Health for partial support of this project (NIH R15 CA91856-01A1). A.B. thanks the McMaster Endowment for research fellowship.

Supporting Information Available: Tables S1–S4 of rate data and Gaussian 98 output files for quantum-mechanical calculations (PDF). This material is available free of charge via the Internet at <http://pubs.acs.org>.

JA037637D